

Sensitivity of different convection schemes in RegCM4.4 for seasonal forecast of temperature and precipitation through winter and summer seasons of 2014 over Egypt

Awatif Ebrahim¹, Tarek Sayad², Sherien A. Zahran³, and Fathy M. El-Hussainy²

¹Egyptian Meteorological Authority, Cairo, Egypt.

²Astronomy and Meteorology Department, Faculty of Science, Al Azhar University, Cairo, Egypt.

³PhD, Researcher, Environment and climate change Research Institute (ECRI), National water research center (NWRC) Ministry of Irrigation and water resources (MIWR), Cairo, Egypt.

Assistance Professor at Canadian International Collage (CIC)

shereinzahran@gmail.com sherine_zahran@cairo-cic.com

Abstract: The mechanism of seasonal climate forecast and early warning is clearly insignificant. It has a great effect on the country's risk management preparedness and socio-economic sectors such that water resources, energy, agricultural, health, and tourism and protection strategies of disasters as well. Seasonal forecasts of rainfall and temperature could be assist in planning, management and mitigate decisions for the policymakers. This research study the long-range seasonal forecast for Egypt, which is conducted with the latest version of the International Centre for Theoretical Physics by using the "Regional Climate Model (RegCM4.4)" driven by Climate Forecast System (CFS) boundary conditions at a grid spacing of 30 km. The Community Land Model; Biosphere-Atmosphere Transfer Scheme (BATS) is used to describe land surface processes. The simulation with Emanuel, Grell and Kain-Fritsch convection schemes are compared against the observations of surface air temperature and precipitation factors because of rectification of the model with focus on these factors. Meanwhile the Temperature and precipitation from the ERA-Interim, GPCP, and NCEP/FNL are reanalysis and used in model evaluations. The model evaluation shows that the forecast of temperature over Egypt is better demeanor in June-July-August (JJA) than in December-January-February (DJF). In DJF a warm bias was found at low south of Egypt. Whatever it was underestimated for precipitation in the north of Egypt and overestimated in south; especially by using Emanuel Scheme. Wherever, by using ERA-Interim reanalysis the predicting of temperature and precipitation were decreased. In addition to the verification process during the summer and winter seasons show that, the maximum root mean square error are decreased.

[Awatif Ebrahim, Tarek Sayad, Sherien A. Zahran and Fathy M. El-Hussainy. **The sensitivity of different convection schemes in RegCM4.4 for seasonal forecast of temperature and precipitation through winter and summer seasons of 2014 over Egypt.** *Life Sci J* 2019;16(4):76-88]. ISSN: 1097-8135 (Print) /ISSN: 2372-613X (Online). <http://www.lifesciencesite.com>. 10. doi: [10.7537/marslsj160419.10](https://doi.org/10.7537/marslsj160419.10).

Keywords: Seasonal variability, Regional climate model, schemes, Egypt

1. Introduction

Egypt's climate profile is hot, dry, deserted and is getting warmer. During the winter season (December– February), Lower Egypt's climate is mild with some rain, primarily over the coastal areas, while Upper Egypt's climate is practically rainless with warm sunny days and cool nights. During the summer season (June- August), the climate is hot and dry all over Egypt. Summer temperatures are extremely high, reaching 38°C to 43°C with extremes of 49°C in the southern and western deserts. The northern areas on the Mediterranean coast are much cooler, with a maximum of about 32°C, see Figure -1-a, (NWRP 2005).

The temperature and precipitation climatology of Egypt is seasonal variability. Most of precipitation occurs in the winter season. The warmest season is in the summer time, while the coldest is in the winter time. Forecasting of precipitation and temperature ahead of few weeks or even a season is critically

important for early warning and decision making in Egypt. Seasonal forecasts are very important in planning of socio-economic sectors such as agriculture, water resources and health. Statistical or dynamical methods are used for seasonal forecasts and sometimes, the combination of both. In this research, the dynamical method is undertaken. It is often used models based on momentum equations.

Global circulation models (GCMs) are used not only to learn about the state of the global climate but can also be used in forecasts. It need high requirement and computational powerful. It comes at high cost. This is one of the most important imperfections of the GCMs. The GCMs often run with low Horizontal resolutions in which influence of high terrain and sub-grid scale processes. Therefore, one way of getting around such a problem is to center on limited areas, leading to apply the regional climate models (RCMs) to get more fine resolutions.

RCMs can perform high-resolution seasonal

predictions with a relatively low price of computational power. Seasonal forecasts Operation provided by the National Centers for Environmental Prediction Weather Service/NOAA/U.S., and (NCEP/FNL) Climate Forecast System (CFS) are perhaps the most used seasonal products obtainable in real time (Saha et al. 2010). The CFS consists of 6-months forecasts available daily with 6-hourly outputs and serves a large range of downscale seasonal implementation. Regional climate models (RegCM4s) have long been used to downscale global climate simulations. However, the ability of RegCM4s to downscale seasonal climate forecasts has received little attention.

In this research, the version four of the Regional Climate Model (RegCM4) was used to give experimental real-time seasonal forecasts of temperature and precipitation for the year 2014 throughout winter and summer season in Egypt area. The RegCM model was based on the Fourth-Generation Miso scale Model developed in the 1980s (Dickinson et al. 1989, Giorgi&Bates 1989, Giorgi et al. 1993a, b). Additional developments and implementation of physical processes have been carried out since the first release of RegCM4 (Giorgi et al., 2012). The version used in this study is RegCM4 (<http://gforge.ictp.it/gf/project/regcm/>). RegCM4 was a hydrostatic version in the vertical sigma sigma-p coordinate that shared many features of the hydrostatic version of the fifth-generation Pennsylvania State/NCAR University National Center for Atmospheric Research Miso-scale Model (MM5; Grell et al. 1994). Many basic variations compared to MM5 include the radiation parameterizations, the land surface scheme, and convective schemes (Elguindi et al. 2004). The improvements in the RegCM model included a new number of physics packages that were introduced on physics schemes of the Climate Model, including new aerosol radiate transfer computations. Recently prognostic equation for cloud water, and a new land surface parameterization are used (see, e.g. Pal et al. 2007, Solmon et al. 2008, Elguindi et al. 2011, Giorgi&Anyah 2012, Giorgi et al. 2012 for more details). Number of observed stations were selected to detect and evaluate the model performance seasonally at different climate pattern all over Egypt.

2. Methodology and Model Setup

In real-time forecasts for all experimental, RegCM4 is configured with a horizontal grid point spacing of 30 km, 18 vertical sigma levels, and the model top at 10 hpa. The model domain is centered at 22° N, 35° E, and consists of 160 grid points in the north-south direction, and 120 grid points east-west, spanning an area from 15 to 55.5° E and 0.0° to 43° N (Fig. 1-b). The model time step was set to 60 s. Model

physics schemes used in this study consist of: 1. the Community Climate Model Version 3 (CCM3) radiation transfer scheme; 2. The land surface scheme (biosphere-Atmosphere Transfer Scheme) (BATS), and 3. The Emanuel, Grell, and Kain-Fritsch convection parameterization schemes. The experiments were conducted during the 2013/2014 winter and 2014 summer season using the regional climate model (RegCM4) to downscale the global CFS outputs, which were provided at real-time by NCEP at the horizontal resolution of $1 \times 1^\circ$. The experiments were designed with the main focus on the 3, and 4 months forecasts of temperature and precipitation, were configured with a single domain as mentioned above.

Forecasts began at 00:00 h UTC November 1, 2013, for winter, and 00:00 h UTC May 1, 2014, for the summer season. Lateral boundary conditions, including the SST, were updated every six hours from the CFS forecasts. Each 6-month forecast generated a 6-hourly 3-dimensional output consisting of horizontal winds, potential temperature, the sea level pressure, and Geo-potential height on the pressure surfaces.

Number of observed stations as shown in tables 1,2,3 were selected to detect and evaluate the model performance seasonally at different climate pattern all over Egypt.

The statistical methods that have been used in this research to evaluate the performance of the model are; Mean Absolute Error (MAE); Bias, and Root-Mean-Square Error (RMSE); as a standard metric for model errors (e.g., McKeen et al., 2005; Savage et al., 2013; Chai et al., 2013) detection of the seasonal changes between model simulation and observed for different stations all over Egypt in term of mean temperatures and precipitations are presented, where:

$$\begin{aligned} \text{RMSE} &= \sqrt{\frac{1}{n} \sum_{i=1}^n (Y_i - \hat{Y}_i)^2} \\ \text{MAE} &= \frac{1}{n} \sum_{i=1}^n |Y_i - \hat{Y}_i| \\ \text{BIAS} &= \frac{1}{n} \sum_{i=1}^n (Y_i - \hat{Y}_i) \end{aligned}$$

In which \bar{Y} is the mean of the data Y_1, \dots, Y_n , $\bar{\hat{Y}}$ is the mean of the predicted values $\hat{Y}_1, \dots, \hat{Y}_n$; and n is the sample size.

2.1 Convective Precipitation Schemes

The convective precipitation parameterizations used in this study are the Tiedtke (1989), Emanuel (1991) and Grell (1993) schemes. The Emanuel (1991) scheme assumes that the mixing in clouds is highly episodic and inhomogeneous (in contrast to a continuous entraining plume) and takes into account convective. Fluxes based on an idealized model of

sub-cloud-scale updrafts and downdrafts. Convection is triggered when the level of neutral buoyancy is greater than the cloud base level. Between these two levels, air is lifted and a fraction of the condensed moisture forms precipitation, while the remaining fraction forms the cloud. The cloud is supposed to mix with the air from the environment according to a uniform spectrum of mixtures that ascend or descend to their respective levels of neutral buoyancy. The mixing entrainment and detrainment rates depend on the vertical gradients of buoyancy in clouds. The Emanuel scheme includes a formulation of the auto-conversion of cloud water into precipitation inside cumulus clouds.

In the Grell (1993) scheme, deep convective clouds are represented by an updraft and a downdraft that are undiluted and mix with environmental air only in the cloud base and top. Heating and moistening profiles are derived from latent heat released or absorbed, linked with the updraft– downdraft fluxes and compensating motion (Martinez-Castro et al., 2006). Two types of Grell scheme convective closure assumptions can be found in RegCM4. In the Arakawa– Schubert (1974) closure (AS), a quasi-equilibrium condition is assumed between the generation of instability by grid scale processes and the dissipation of instability by sub-grid (convective) processes. In the Fritsch–Chappell (FC) closure (Fritsch and Chappell, 1980), the available buoyant energy is dissipated during a specified convective time period (between 30 min and 1 h). Similarly, the Tiedtke (1989) scheme is a mass flux convection scheme, although it considers a number of cloud types as well as cumulus downdrafts that can represent deep, mid-level and shallow convection (Singh et al., 2011; Bhatla et al., 2016). The closure assumptions for the deep and midlevel convection are maintained by large-scale moisture convergence, while the shallow convection is sustained by the supply of moisture derived from surface evaporation.

2.2 Data treated

NCEP FNL (Final) Operational Global Analysis data are on 1-degree by 1-degree grids prepared operationally every six hours. This product is from the Global Data Assimilation System (GDAS), which constantly collects observational data from the Global Tele-connections System (GTS), and other sources, for many analyses. The FNLs are made with the same model that the NCEP uses in the Global Forecast System (GFS), but the FNLs are prepared about an hour or so after the GFS is initialized. The FNLs are delayed so that more observational data can be used. The GFS runs previously in upholding critical time forecast necessarily and uses the FNL from the previous 6-hour cycle as part of its initialization. This data of NCEP FNL is located at <[\[car.edu/datasets/d_s083.2/\]\(https://rda.car.edu/datasets/d_s083.2/\).](https://rda.</p>
</div>
<div data-bbox=)

One degree daily (1DD) precipitation data from Global Precipitation Climatology Project (GPCP) is obtained. 1DD GPCP data is available at 1° grid spacing on daily basis from 1996-present. Rainfall data is prepared on pentad and season basis. The daily, pentad and seasonal precipitation data is compatible to estimates of the combined computation from sounder, infrared and microwave data observed by the international satellite constellation related to precipitation, and rainfall gauge analyzes. It is to be noted that due to a hardware failure; GPCP SG V2.2 and One-Degree Daily V1.2 have ceased production (Huffman, G. J., and Coauthors, 1997). The last processed month is October 2015. This data set is available at <https://precip.gsfc.nasa.gov/>.

ERA-Interim is a major commitment by European Centre for Medium-Range and Weather Forecasts (ECMWF) to reproduce a reanalysis with an improvement atmospheric model and assimilation system. These data was applied to replace those used in ERA-40, especially for the data-rich 1990s and 2000s, to continue as a system ECMWF's, meanwhile Climate Data Acquisition (ECDAS) will be replaced.

Initial operation indicated that many of the inaccuracies shown by the ERA-40, such as the very strong precipitation of the oceans from the early 1990s onwards and the Brewer-Dobson circulation are very strong in the stratosphere, have been largely eliminated or reduced. The production of ERA-Interim began in 1989 and onwards in the summer of 2006. (The period from 1979 to 1988 was used in advance in 2011). The ERA-Interim data set is used at 1° × 1° to obtain initial and time-evolving lateral boundary stipulation at intervals of time every 6-hour to run the form that initial and time-improve lateral boundary conditions at six-hourly intervals to drive the model. This data of ERA-Interim is located at <https://www.ecmwf.int/en/forecasts/datasets>.

3. Results

Egypt is dominated by its hot and dry climate during the summer season between May and October. The annual average temperatures in the coastal regions range between (14 - 37) °C. While the desert areas exhibit greater variations, the maximum day temperature is around 46°C and drops to minimums of around 6°C during nighttime. The area along the Mediterranean coast has high humidity levels and an annual rainfall of about 200mm, while precipitation rapidly decreases southwards.

Using RCM CM 4.4, spatial distribution in December, January, and February (DJF) and June, July, and August (JJA) were analyzed for mean Temperature and Precipitation. Fig. 1-b show model topography for RegCM4 domain (m), meanwhile the

results are presented in detailed next section:

3.1 Mean Temperature in DJF

Regarding to the mean temperature, Fig. 2 and table (1) show the bias at DJF (model minus observations NCEP/FNL) of the RegCM4 simulation using Emanuel Scheme, Grell Scheme, and Kain-Fritsch Scheme, as well as the bias (model minus observations ERA-Interim) with the same Schemes. In general the model is too warm over Egypt in DJF, except the Red Sea (Fig. 2a, b, c, d, e, and f). It is noted that the general warm bias from the field of the ERA-Interim is decreased compared to observed reanalysis data from NCEP/FNL (Fig. 2 d, e, and f). The bias is equal to model minus observations, at DJF for ERA-Interim is typically in the range of -1.98°C to 4.94°C (-0.02°C to 4.23°C) by using Emanuel, -2.89°C to 4.99°C and (-0.94°C to 4.28°C) by using Grell, and -2.05°C to 4.73°C (-0.09°C to 4.02°C) using Kain-Fritsch Scheme, and the bias greater than 4.99°C in the southern Egypt and less than -2.89°C at the red sea (Fig. 2a, b, and c), and table (1). The model is too warm over the deserts in southwest Egypt, and the best simulation for the 12 stations was within the previous version Kain-Fritsch Scheme as shown in Fig. 2c, f, and table (1), as of RegCM4 (e.g., Zhang et al., 2008). The maximum root mean square error (RMSE) for 12 stations was at 6.42 for Kharga (25.45°N 30.53°E) and the minimum root mean square error (RMSE) 2.84 Dabaa region (30.93°N 28.46°E) as shown in table (1), and Figure 3a, and b.

The prevailing warm bias over the high latitudes in the cold seasons can also be found in different generations of GCM simulations (e.g., Xu et al., 2010; Jiang et al., 2016). However, large uncertainties in the observation data exist in this largely uninhabited region, which is characterized by a sparse station distribution. Analysis has shown that the temperature differences among different gridded datasets can be up to several degrees over the region (Wu and Gao, 2013; Sun et al., 2014).

3.2. Mean Temperature in JJA

In JJA, temperature from the RegCM4 simulation is in good agreement with observations. The model is in general warm over Egypt in JJA, except Mediterranean and red Sea (Fig. 4 a, b, c, d, e and f). The bias model minus observations NCEP/FNL (model minus ERA-Interim) during JJA is typically in the range of -2.43°C to 3.22°C (-2.39°C to 2.37°C)

using Emanuel, -2.43°C to 3.41°C (-2.38°C to 2.19°C) using Grell, and -2.43°C to 2.84°C (-2.39°C to 2.01°C) using Kain-Fritsch Scheme, and temperature greater than 3.41°C in southern Egypt, and less than -2.34°C on Mediterranean and red Sea as shown in table 2. The maximum root mean square error for the 12 stations was 4.23 for Kharga (25.45°N 30.53°E), and the minimum root mean square error (RMSE) 1.69 Port Said (31.26°N 32.29°E) as shown in table (2), and Figure 5a, and b.

3.3 Mean Precipitation in DJF

Significant amounts of December-to-February (DJF) seasonal rainfall over Egypt are mainly received in parts of northern Egypt. In DJF, precipitation of the model RegCM4 is in general dry over Egypt in DJF except some parts of the red sea, (Fig. 6 a, b, c, d, e and f). The bias model minus observations (model minus ERA-Interim) during DJF is range of -0.68 mm/day to 0.48 mm/day (-1.38 mm/day to 0.55 mm/day) using Emanuel, -0.95 mm/day to 0.05 mm/day (-1.56 mm/day to 0.13 mm/day) using Grell, and -0.98 mm/day to 0.00 mm/day (-1.58 mm/day to 0.03 mm/day) using Kain-Fritsch Scheme, and precipitation less than -1.58° mm/day on the Mediterranean sea, and greater than 0.55 mm/day on the red Sea as shown in table (4.3). The maximums and the minimums root mean square error are presented at table (3) and figure 7a, and b for example it was 4.2 Alexandria (3.25°N , 29.95°E), and 0.02 in Kharga (25.45°N 30.53°E).

3.4 Mean Precipitation in JJA

In JJA, precipitation from the RegCM4 simulation is in good agreement with observations for the most of Egypt. The model is wet over the red Sea and south Egypt (Fig. 4 a, b, c, d, e and f). The bias model minus observations NCEP/FNL (model minus ERA-Interim) during JJA is typically in the range of -0.05 mm/day to 0.36 mm/day (-0.05 mm/day to 0.36 mm/day) using Emanuel, -0.04 mm/day to 0.06 mm/day (-0.05 mm/day to 0.06 mm/day) using Grell, and -0.05 mm/day to 0.54 mm/day (-0.06 mm/day to 0.14 mm/day) using Kain-Fritsch Scheme, and precipitation greater than 0.54 mm/day in southern Egypt, and less than -0.06 mm/day on Mediterranean Sea as shown in table 2. The maximum root mean square error for the 12 stations was 2.46 for Hurguada (27.15°N 33.71°E), and the minimum root mean square error (RMSE) 0.00 Kharga (25.45°N 30.53°E) as shown in table (4), and Figure 9a, and b.

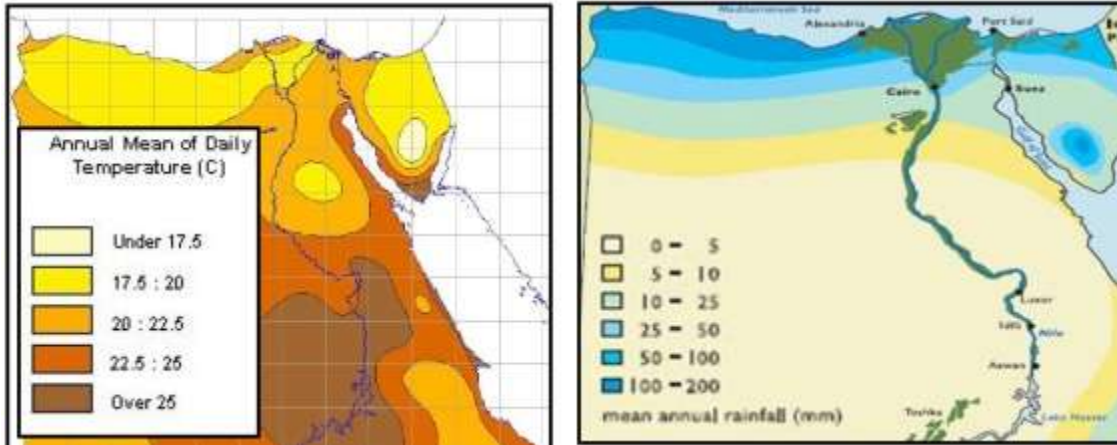


Figure 1a: The average annual temperature across Egypt from 1961 to 2000 and b: the average annual precipitation (NWRP 2005).

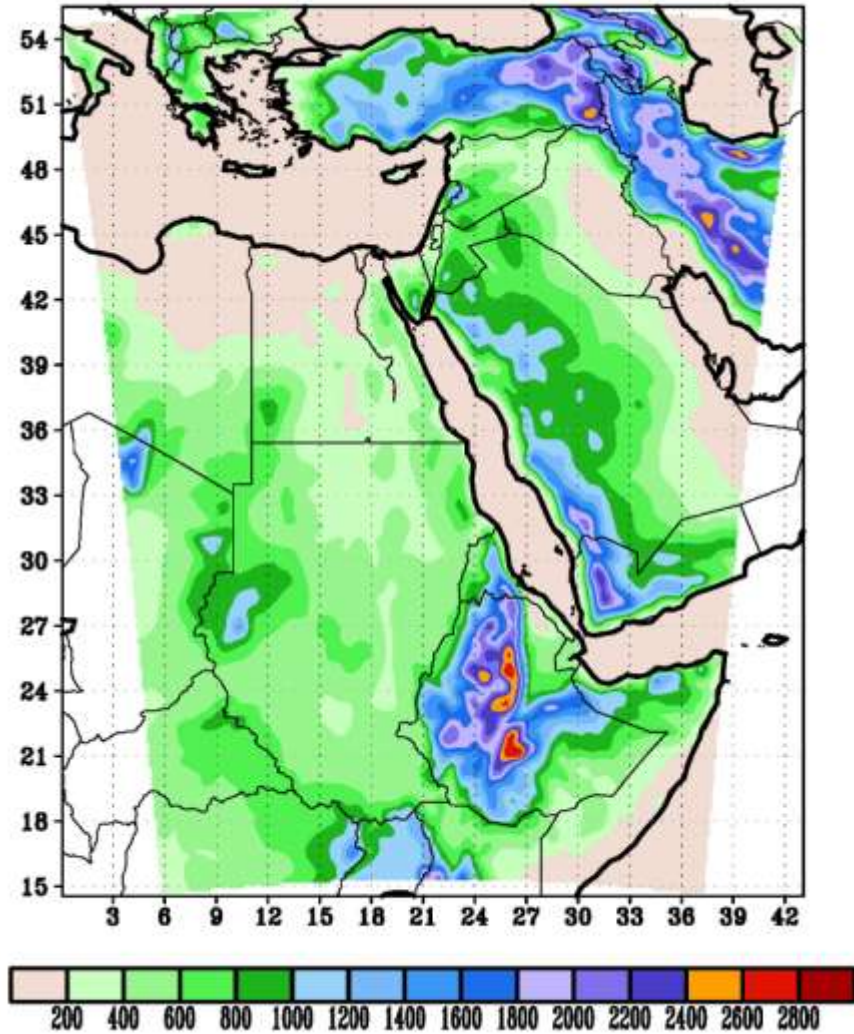


Fig. 1-b: Model Topography for Regcm4 Domain (M).

Table (1) Errors of mean temperature over different Egyptian stations in DJF.

stations	Emanuel				Grell				Kain-Fritsch			
	FNL		ERA		FNL		ERA		FNL		ERA	
	Bias	RMSE	Bias	RMSE	Bias	RMSE	Bias	RMSE	Bias	RMSE	Bias	RMSE
MersaMatruh Lat. 1.33 Lon. 27.21 Alt. 25	3.49	23	3.5	23	2.96	3.9	2.96	3.91	3.13	3.97	3.14	3.96
Dabaa Lat. 30.93 Lon. 28.46	1.4	2.93	1.66	2.96	0.84	2.89	1.1	2.87	0.87	2.87	1.13	2.84
Alexandria Lat. 31.2 Lon. 29.95	3.37	22	3.24	09	2.9	3.95	2.78	3.83	3.22	15	3.1	02
Port Said Lat. 31.26 Lon. 32.29	3.61	63	3.79	75	3.03	33	3.21	42	3.27	41	3.45	51
El Arish Lat. 31.08 Lon. 33.83	1.66	3.72	06	5.25	0.95	3.61	3.34	81	0.89	3.53	3.28	73
Cairo Lat. 30.13 Lon. 31.4	2.27	2	2.38	24	1.87	18	1.98	22	2.05	19	2.16	22
Minya Lat. 28.08 Lon. 30.73	3.96	5.32	3.74	5.05	3.81	5.31	3.59	5.04	3.82	5.26	3.59	99
Asyut Lat. 27.05 Lon. 31.01	86	6.06	3.82	5.12	55	5.92	3.51	5.01	54	5.87	3.5	95
Luxor Lat. 25.66 lon. 32.7	61	6.03	3.15	59	13	5.71	2.67	33	07	5.67	2.62	28
Aswan Lat. 23.96 Lon. 32.78	09	5.78	1.51	13	3.77	5.61	1.18	1	3.89	5.68	1.3	12
Hurguada Lat. 27.15 Lon.33.71	-1.98	3.51	-0.02	2.93	-2.89	25	-0.94	3.24	-2.05	3.67	-0.09	3.04
Kharga Lat. 25.45 Lon. 30.53	94	6.36	23	5.7	99	6.42	28	5.75	73	6.22	02	5.57

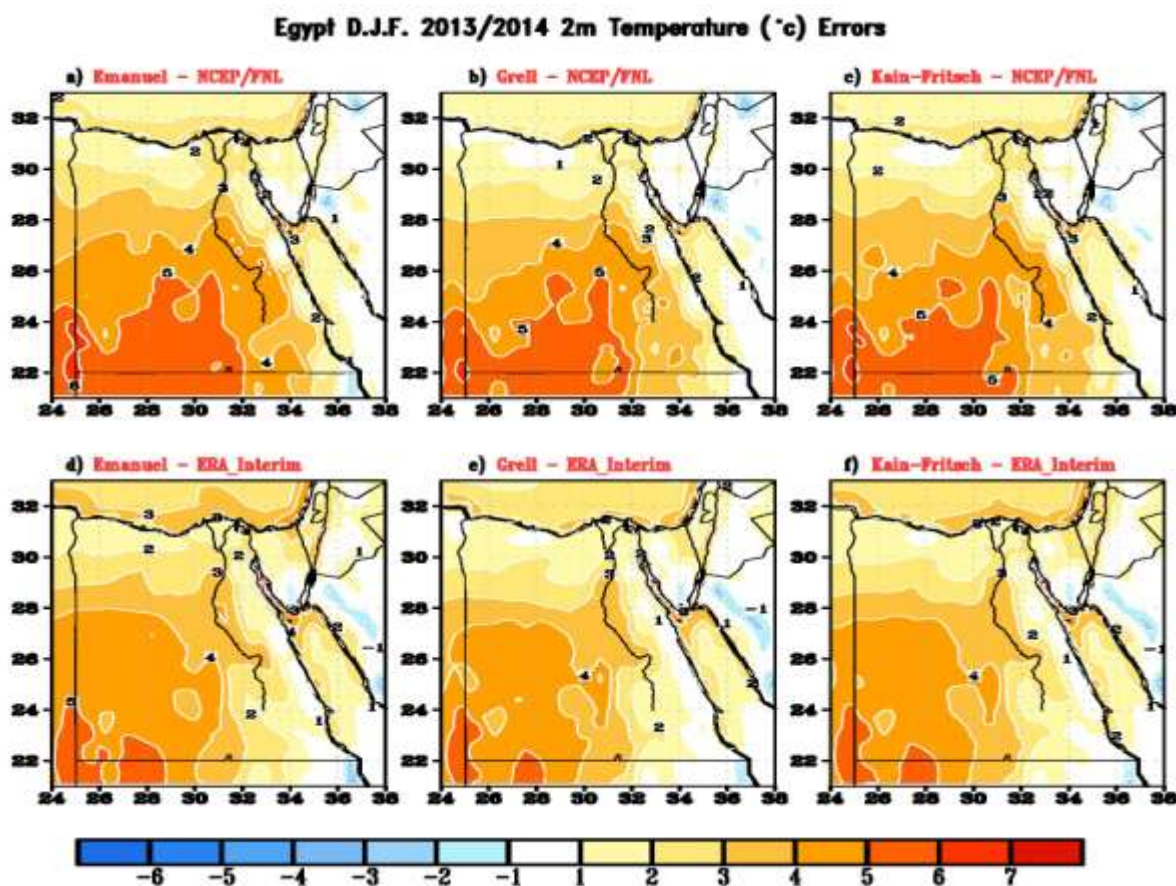


Fig. 2: Differences between RegCM4 simulated over Egypt using Emanuel, Grell, and Kain-Fritsch Scheme during DJF 2013/2014, and NCEP/FNL (a,b,c) at the top and ERA-Interim (d,e,f) down Reanalysis (observed) at the bottom at 2m Temperature (°C) respectively.

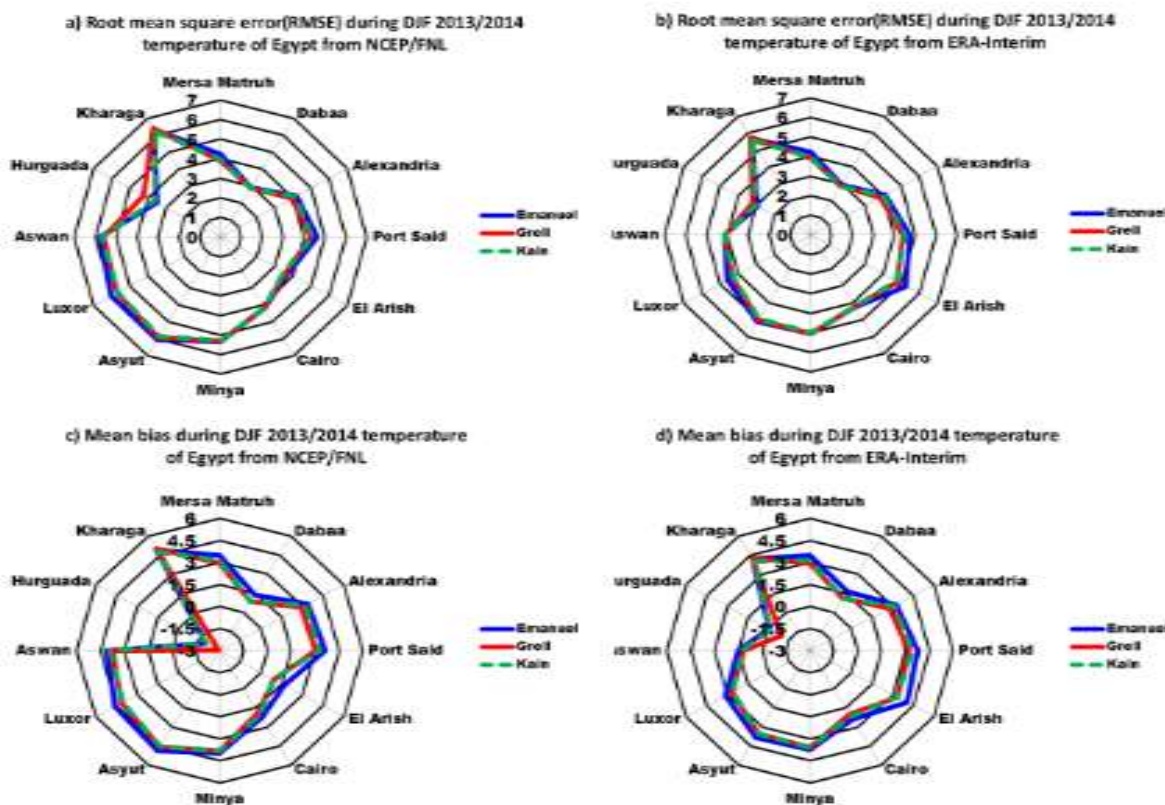


Fig. 3(a,b, c, and d), Spatial root-mean-square error (RMSE) and Spatial mean bias error (ME), for different stations, between RegCM4 simulation over Egypt during DJF 2013/2014, and NCEP/FNL & ERA-Interim at 2m Temperature (°C) respectively.

Table (2) Errors of mean temperature over different Egyptian stations in JJA.

stations	Emanuel		Grell		Kain-Fritsch							
	FNL		ERA		FNL		ERA					
	Bias	RMSE	Bias	RMSE	Bias	RMSE	Bias	RMSE				
MersaMatruh 27.21 Alt. 25 Lat. 1.33, Lon.	-1.47	2.54	-1.83	2.65	-1.54	2.66	-1.9	2.78	-1.67	2.65	-2.03	2.78
Dabaa Lat. 30.93 Lon. 28.46	1.43	2.71	2.17	3.07	1.29	2.68	2.03	2.99	0.85	2.46	1.59	2.68
Alexandria Lat. 31.2 Lon. 29.95	-2.43	2.89	-2.39	2.77	-2.43	2.91	-2.38	2.8	-2.43	2.9	-2.39	2.79
Port Said Lat. 31.26 Lon. 32.29	-0.42	1.69	-1.08	1.89	-0.48	1.71	-1.14	1.92	-0.75	1.83	-1.4	2.1
El Arish Lat. 31.08 Lon. 33.83	0.96	2.35	0.94	2.22	0.71	2.25	0.69	2.13	0.74	2.24	0.72	2.1
Cairo Lat. 30.13 Lon. 31.4	1.61	3.01	1.43	2.8	1.61	2.98	1.42	2.76	1.29	2.8	1.1	2.6
Minya Lat. 28.08 Lon. 30.73	1.43	2.71	2.17	3.07	1.29	2.68	2.03	2.99	0.85	2.46	1.59	2.68
Asyut Lat. 27.05 Lon. 31.01	-2.43	2.89	-2.39	2.77	-2.43	2.91	-2.38	2.8	-2.43	2.9	-2.39	2.79
Luxor Lat. 25.66 lon. 32.7	2.71	3.5	0.83	2.48	2.17	3.1	0.29	2.3	2	3	0.12	2.33
Aswan Lat. 23.96 Lon. 32.78	2.76	3.51	0.47	2.19	2.33	3.23	0.05	2.2	1.65	2.75	-0.63	2.28
Hurguada Lat. 27.15 Lon. 33.71	2.57	3.34	-1	2.43	2.57	3.31	-1	2.39	2.49	3.22	-1.08	2.39
Kharga Lat. 25.45 Lon. 30.53	3.22	13	2	3.39	3.41	23	2.19	3.44	2.84	3.86	1.62	3.19

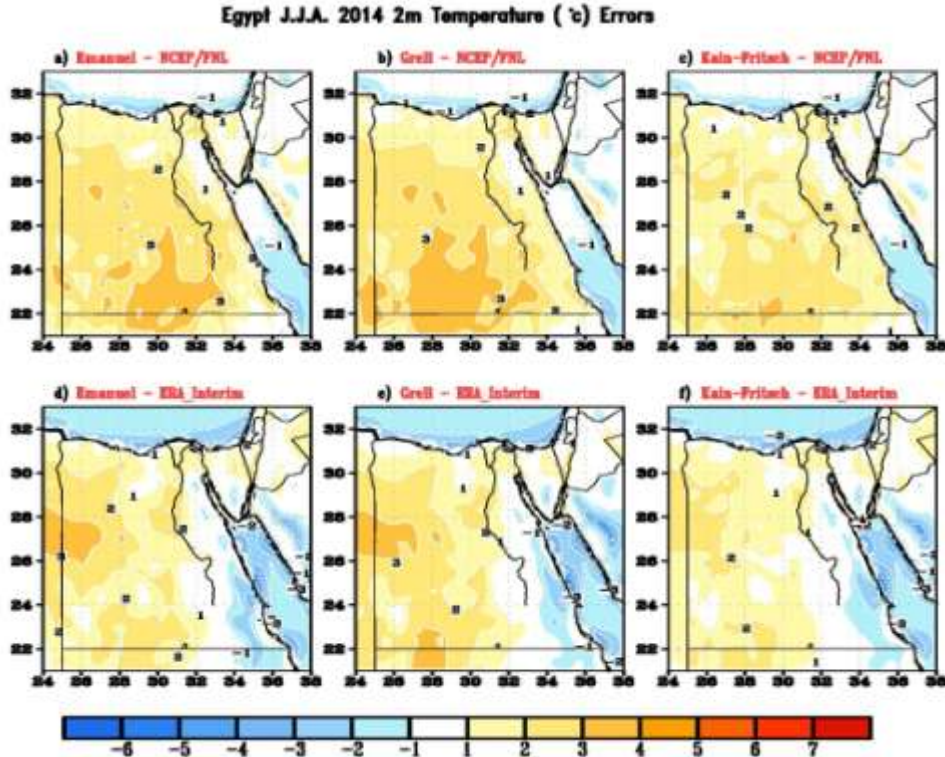


Fig. 4: Differences between RegCM4 simulated over Egypt using Emanuel, Grell, and Kain-Fritsch Scheme during JJA 2014, and NCEP/FNL (a,b,c) at the top and ERA-Interim (d,e,f) down Reanalysis (observed) at the bottom at 2m Temperature (°C) respectively.

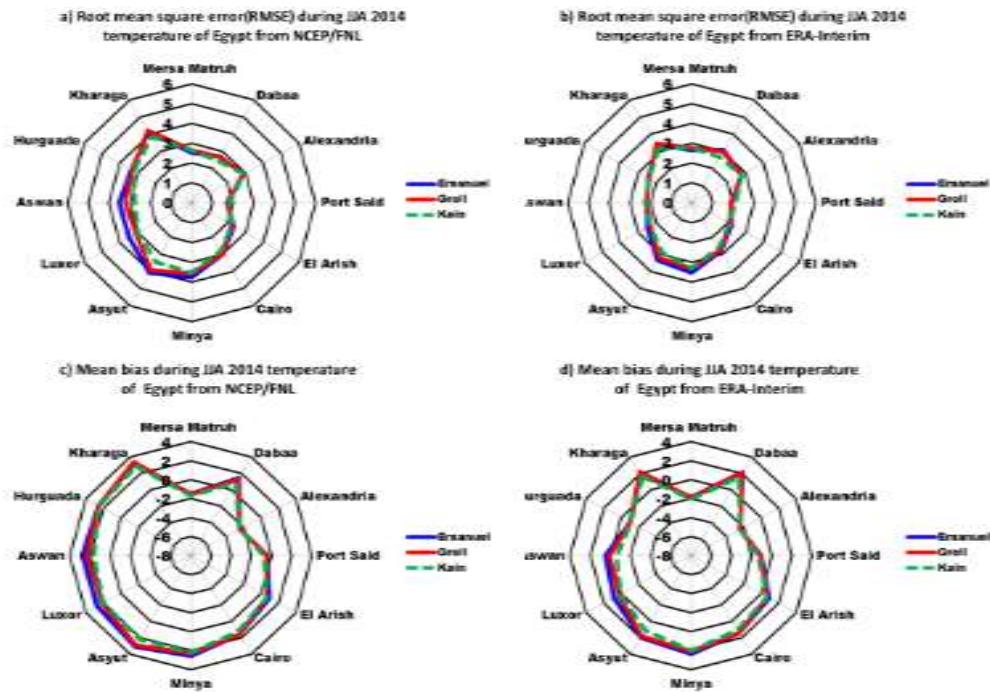


Fig. 5 (a,b, c, and d), Spatial root-mean-square error (RMSE) and Spatial mean bias error (ME), for different stations, between RegCM4 simulation over Egypt during JJA 2014, and NCEP/FNL & ERA-Interim at 2m Temperature (°C) respectively.

Table (3) Errors of accumulate Precipitation over different Egyptian stations in DJF.

stations	Emanuel				Grell				Kain-Fritsch			
	FNL		ERA		FNL		ERA		FNL		ERA	
	Bias	RMSE	Bias	RMSE	Bias	RMSE	Bias	RMSE	Bias	RMSE	Bias	RMSE
MersaMatruh Lat. 1.33 Lon. 27.21Alt. 25	-0.57	8	-0.07	1.78	-0.89	3.99	-0.39	1.63	-0.94	3.97	-0.44	1.56
Dabaa Lat. 30.93 Lon. 28.46	-0.24	2.91	-1.38	3.38	-0.42	2.88	-1.56	3.44	-0.44	2.87	-1.58	3.43
Alexandria Lat. 31.2 Lon. 29.95	-0.32	2	-0.76	3.38	-0.8	3.94	-1.25	3.31	-0.88	3.92	-1.33	3.28
Port Said Lat. 31.26 Lon. 32.29	-0.37	3.1	-0.17	2.11	-0.68	3.01	-0.48	2.11	-0.81	2.96	-0.61	2.01
El Arish Lat. 31.08 Lon. 33.83	-0.68	3.38	-0.89	3.77	-0.95	3.31	-1.16	3.73	-0.98	3.31	-1.19	3.72
Cairo Lat. 30.13 Lon. 31.4	-0.34	2.49	-0.08	1.23	-0.51	2.43	-0.25	1.12	-0.49	2.43	-0.24	1.16
Minya Lat. 28.08 Lon. 30.73	-0.11	0.66	-0.03	0.56	-0.12	0.7	-0.04	0.62	-0.14	0.63	-0.06	0.52
Asyut Lat. 27.05 Lon. 31.01	-0.06	0.32	0	0.15	-0.07	0.32	-0.02	0.14	-0.07	0.32	-0.01	0.16
Luxor Lat. 25.66 lon. 32.7	0.04	0.26	0.05	0.3	-0.01	0.04	0.01	0.07	-0.01	0.05	0	0.01
Aswan Lat. 23.96 Lon. 32.78	-0.01	0.14	0.01	0.05	-0.02	0.15	0.01	0.07	-0.02	0.13	0	0
Hurguada Lat. 27.15 Lon.33.71	0.48	3.5	0.55	3.67	0.05	0.67	0.13	0.61	-0.04	0.42	0.03	0.22
Kharga Lat. 25.45 Lon. 30.53	0.01	0.06	0.01	0.05	0	0.02	0	0	0	0.02	0	0

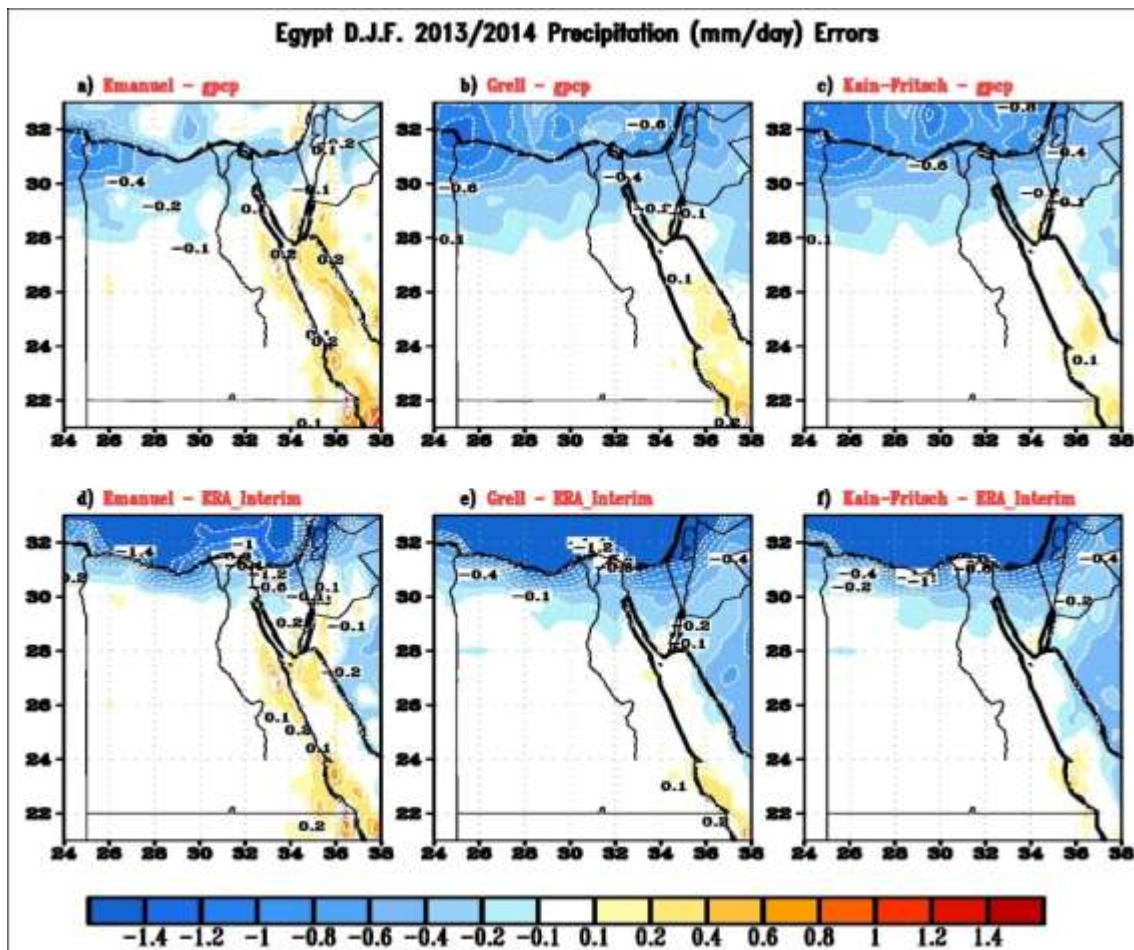


Fig. 6: Differences between RegCM4 simulation over Egypt using Emanuel, Grell, and Kain-Fritsch Schemes during JJA 2014, and GPCP(a,b,c) at the top and ERA-Interim down re-analysis (observed) precipitation rates (mm/day) (d,e,f) at the bottom; respectively.

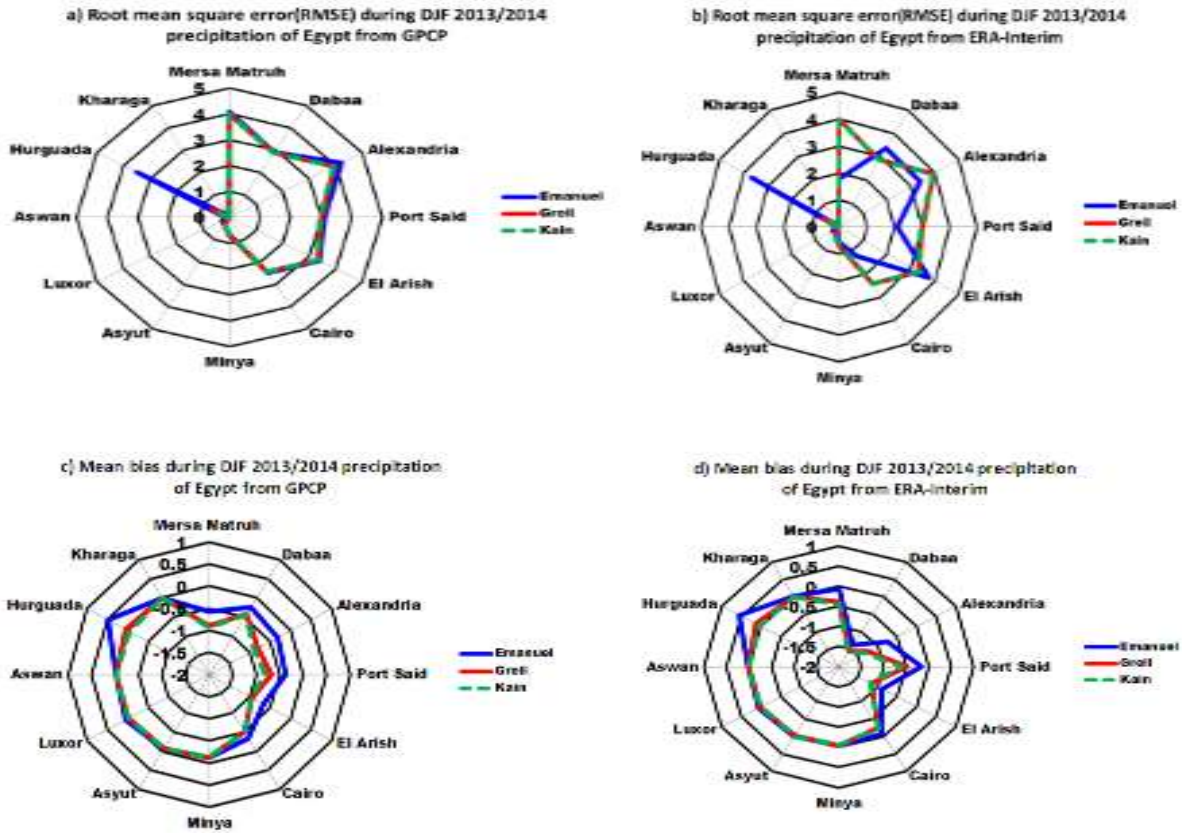


Fig. 7 (a, b, c, and d), Spatial root-mean-square error (RMSE) and Spatial mean bias error (ME), for different stations, between RegCM4 simulation over Egypt during DJF 2013/14, and observed reanalysis precipitation (GPCP), & precipitation ERA-Interim respectively.

Table (4) Errors of accumulate Precipitation over different Egyptian stations in JJA.

stations	Emanuel				Grell				Kain-Fritsch			
	FNL		ERA		FNL		ERA		FNL		ERA	
	Bias	RMSE	Bias	RMSE	Bias	RMSE	Bias	RMSE	Bias	RMSE	Bias	RMSE
MersaMatruh Lat. 1.33 Lon. 27.21 Alt. 25	-0.03	0.16	-0.01	0.08	-0.02	0.17	0	0.1	-0.03	0.16	-0.01	0.08
Dabaa Lat. 30.93 Lon. 28.46	-0.01	0.04	0	0	0.04	0.29	0.05	0.28	-0.01	0.04	0	0
Alexandria Lat. 31.2 Lon. 29.95	-0.02	0.33	0.01	0.15	-0.02	0.31	0.02	0.12	-0.04	0.29	-0.01	0.04
Port Said Lat. 31.26 Lon. 32.29	-0.05	0.27	-0.03	0.13	-0.04	0.27	-0.02	0.13	-0.05	0.27	-0.03	0.13
El Arish Lat. 31.08 Lon. 33.83	0	0.05	0	0.1	0.01	0.16	0.01	0.17	-0.01	0.07	-0.02	0.07
Cairo Lat. 30.13 Lon. 31.4	0	0.18	0.01	0.16	0.02	0.21	0.03	0.19	-0.02	0.11	-0.01	0.05
Minya Lat. 28.08 Lon. 30.73	0.2	0.95	0.18	0.95	0.04	0.14	0.03	0.15	0.15	0.93	0.14	0.93
Asyut Lat. 27.05 Lon. 31.01	0.01	0.05	0	0.07	0.05	0.37	0.03	0.37	0	0.02	-0.01	0.05
Luxor Lat. 25.66 lon. 32.7	-0.01	0.09	-0.05	0.12	-0.01	0.09	-0.05	0.12	-0.01	0.09	-0.05	0.12
Aswan Lat. 23.96 Lon. 32.78	0.01	0.09	-0.05	0.18	0.01	0.1	-0.05	0.18	0	0.02	-0.06	0.16
Hurguada Lat. 27.15 Lon.33.71	0.36	2.46	0.36	2.46	0.06	0.54	0.06	0.54	0.01	0.08	0.01	0.07
Kharga Lat. 25.45 Lon. 30.53	0.04	0.2	0.05	0.19	-0.01	0.04	0	0	-0.01	0.04	0	0

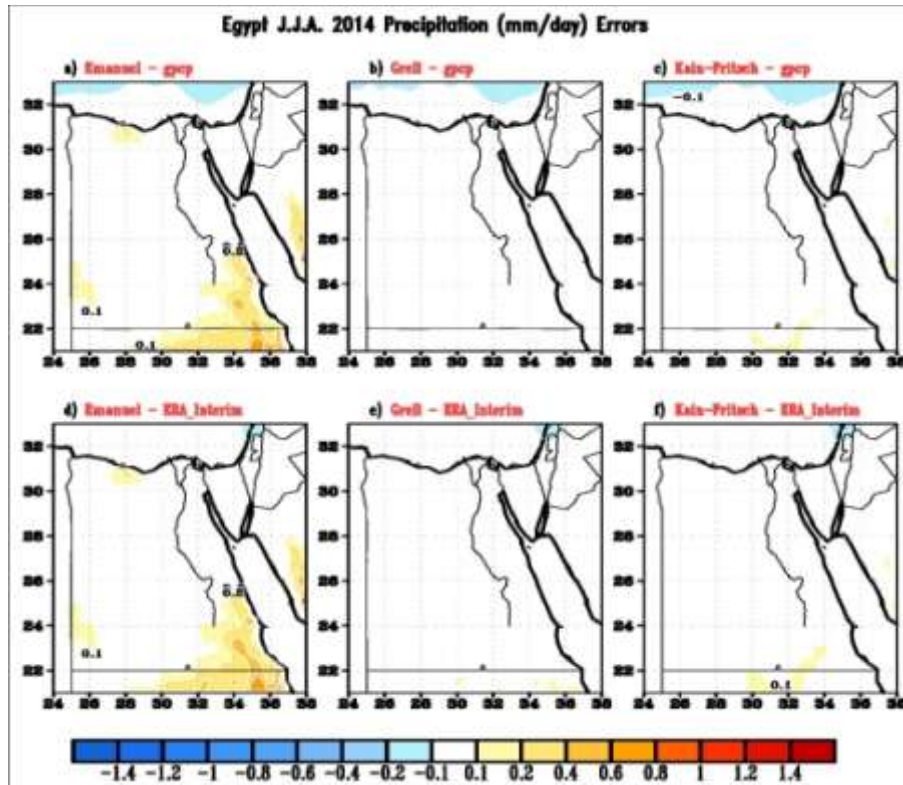


Fig. 8: Differences between RegCM4 simulation over Egypt using Emanuel, Grell, and Kain-Fritsch Schemes during JJA 2014, and GPCP(a,b,c) at the top and ERA-Interim re-analysis (observed) precipitation rates (mm/day) (d,e,f) at the bottom; respectively.

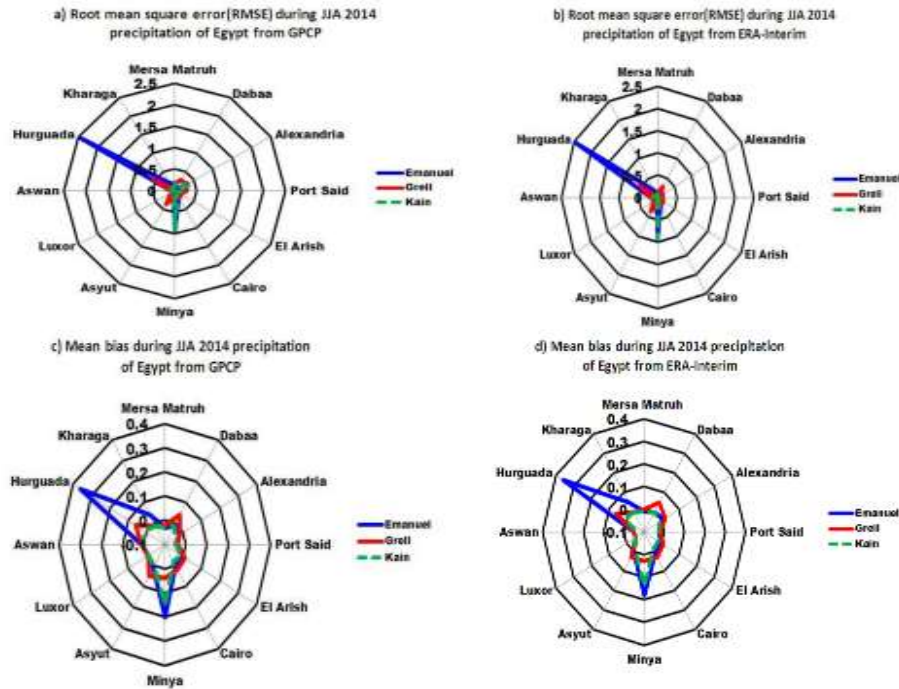


Fig. 7, Spatial root-mean-square error (RMSE) (a&b) at the top and Spatial mean bias error (ME) (C&d) at the bottom, for different stations, between RegCM4 simulation over Egypt during DJF 2013/14, and observed reanalysis precipitation (GPCP), & precipitation ERA-Interim respectively

4. Conclusions and Recommendations

The performance of RegCM4, using BATS as the land surface scheme, over Egypt was reported in this research. The model was driven by Climate Forecast System (CFS) data. DJF, JJA simulation were conducted using a horizontal resolution of 30 km with Emanuel, Grell, and Kain-Fritsch cumulus parameterization schemes. Observations extracted from reanalysis NCEP/FNL, GPCP and ERA-Interim have been used to get the biases of temperature and precipitation at Egypt. It was concluded that, the model biases are smaller in JJA compared to DJF, whenever, a warm bias was in the southern Egypt and cold bias over the Mediterranean and red Sea are found especially during JJA season.

General average precipitation pattern is also reproduced by the model; it was underestimating during DJF and JJA over Egypt in the north, and overestimate in the Red Sea. So, the study recommended that the seasonal variability is reported well for precipitations using the convention scheme of Emanuel, and Grell during the winter and Kain-Fritsch during the summer.

Acknowledgements

Grateful and thanks should be provide to Egyptian meteorological Authority (EMA) staff at Egypt, for their endless support. The authors are grateful to the entire member of The Earth System Physics Research Group of International Centre for Theoretical Physics, Trieste, Italy, for the access granted and the necessary training given on the usage of RegCM 4.4. Also special thanks to Dr. Zinab Salah at EMA, and Dr. Mohammed Sharaf, at UDAF, USA for their kind support.

References

1. Arakawa, A. and Schubert, W. H.: Interaction of a cumulus cloud ensemble with the large scale environment Part I, *J. Atmos. Sci.*, 31, 674–701, 1974.
2. Bhatla, R., Ghosh, S., Mandal, B., Mall, R. K., and Sharma, K.: Simulation of Indian summer monsoon onset with different parameterization convection schemes of RegCM-4.3, *Atmos. Res.*, 176, 10–18, <https://doi.org/10.1016/j.atmosres.2016.02.010>, 2016.
3. Dickinson RE, Errico RM, Giorgi F, Bates GT (1989) a regional climate model for the western United States. *Clim Change* 15: 383–422.
4. Elguindi N, Bi X, Giorgi F, Nagarajan B, Pal J, Solmon F, Giuliani G (2011) Regional climatic model RegCM user manual version 1. ICTP, Trieste.
5. Elguindi N, Bi X, Giorgi F, Nagarajan B, Pal J, Solmon F, Zakey A (2004) RegCM version 3.0 user's guide. The Abdus Salam International Centre for Theoretical Physics (ICTP), Trieste.
6. Emanuel KA (1991) A scheme for representing cumulus convection in large-scale models. *J Atmos Sci* 48(21):2313–2335.
7. Fritsch JM, Chappell CF (1980) Numerical prediction of convectively driven mesoscale pressure systems. Part I: convective parameterization. *J Atmos Sci* 37:1722–1733.
8. Giorgi F, Anyah RO (2012). The road towards RegCM *Clam Res* 52: 3–6.
9. Giorgi F, Bates GT (1989) on the climatological skill of a regional model over complex terrain. *Mon Wea Rev* 117:2325–2347.
10. Giorgi, F., and Coauthors, 2012: RegCM4: Model description and preliminary tests over multiple CORDEX domains. *Climate Research*, 52, 7–29.
11. Giorgi, F., M. R. Marinucci, and G. T. Bates, 1993a: Development of a second-generation regional climate model (RegCM2). Part I: Boundary-layer and radiative transfer processes. *Mon. Wea. Rev.*, 121, 2794–2813.
12. Giorgi, F., M. R. Marinucci, and G. T. Bates, 1993b: Development of a second-generation regional climate model (RegCM2). Part II: Convective processes and assimilation of lateral boundary conditions. *Mon. Wea. Rev.*, 121, 2814–2832.
13. Grell G (1993) Prognostic evaluation of assumptions used by cumulus parameterizations. *Mon Wea Rev* 121:764–787.
14. Grell GA, Dudhia J, Stauffer D R (1994) A description of the fifth-generation Penn State/NCAR mesoscale model (MM5). Technical Note NCAR/TN-398+STR, National Center for Atmospheric Research (NCAR), Boulder, CO.
15. Grell GA, Dudhia J, Stauffer DR (1994) Description of the fifth generation Penn State/NCAR Mesoscale Model (MM5), Tech. Rep. TN-398+STR. NCAR, Boulder, Colorado, p 121.
16. Huffman, G. J., and Coauthors, 1997: The Global Precipitation Climatology Project (GPCP) combined precipitation dataset. *Bull. Amer. Meteor. Soc.*, 78, 5–20. Link, Google Scholar.
17. Martinez-Castro, D., da Rocha, R. P., Bezanilla-Morlot, A., Alvarez-Escudero, L., Reyes-Fernández, J. P., Silva-Vidal, Y., and Arritt, R. W.: Sensitivity studies of the RegCM3 simulation of summer precipitation, temperature and local wind field in the Caribbean Region, *Theor. Appl. Climatology.*, 86, 5–22,

- <https://doi.org/10.1007/s00704-005-0201-9>, 2006.
18. McKeen, S. A., Wilczak, J., Grell, G., Djalalova, I., Peckham, S., Hsie, E., Gong, W., Bouchet, V., Menard, S., Moffet, R., McHenry, J., McQueen, J., Tang, Y., Carmichael, G. R., Pagowski, M., Chan, A., Dye, T., Frost, G., Lee, P., and Mathur, R.: Assessment of an ensemble of seven realtime ozone forecasts over eastern North America during the summer of 2004, *J. Geophys. Res.*, 110, D21307, doi: 10.1029/2005JD005858, 2005.
 19. NWRP-2005; "National Water Resources Plan, Facing the Challenge", Ministry of Water Resources and Irrigation, Integrated Water Resources Management Plan for 2017.
 20. Pal JS, Giorgi F, Bi X, Elguindi N and others (2007) Regional climate modeling for the developing world: the ICTP RegCM3 and Recent. *Bull Am Meteorol Soc* 88: 1395–1409.
 21. Saha S et al (2010) The NCEP climate forecast system reanalysis. *Bull Am Meteorol Soc* 91:1015–1057.
 22. Savage, N. H., Agnew, P., Davis, L. S., Ordóñez, C., Thorpe, R., Johnson, C. E., O'Connor, F. M., and Dalvi, M.: Air quality modeling using the Met Office Unified Model (AQUUM OS24-26): model description and initial evaluation, *Geosci. Model Dev.*, 6, 353–372, doi:10. 5194 / gmd-6-353-2013, 2013.
 23. Singh, A. P., Singh, R. P., Raju, P. V. S., and Bhatla, R.: Comparison of three different cumulus parameterization schemes on Indian summer monsoon circulation, *Int. J. Ocean climate. Syst.*, 2, 27– 43, 2011.
 24. Solmon F, Mallet M, Elguindi N, Giorgi F, Zakey AS, Konare A (2008) Dust aerosol impact on regional precipitation over western Africa, mechanisms and sensitivity to ab -Sorption properties. *Geophys Res Lett* 35: L24705, doi: 10. 1029 /2008 GL 03 5900.
 25. Sylla, M. B., Gaye, A. T., Pal, J. S., Jenkins, G. S., and Bi, X. Q.: High resolution simulations of West Africa climate.
 26. Using Regional Climate Model (RegCM3) with different lateral boundary conditions, *Theor. Appl. Climatol.*
 27. Tiedtke, M.: A Comprehensive Mass Flux Scheme for Cumulus Parameterization in Large-scale Models, *Mon. Weather Rev.*, 117, 1779–1800, 1989.
 28. Tadross, M. A., Gutowski, W. J. Jr, Hewitson, B. C., Jack, C., and New, M.: MM5 simulations of internal change and the diurnal cycle of Southern African regional climate, *Theor. Appl. Climatol.*, 86, 63–80, 2006.

4/19/2019